Proceedings of the ASME 2010 3rd Joint US-European Fluids Engineering Summer Meeting and 8th International Conference on Nanochannels, Microchannels, and Minichannels
FEDSM-ICNMM2010
August 1-5, 2010, Montreal, Canada

FEDSM-ICNMM2010-30910

NUMERICAL MODELING OF MASS TRANSFER THROUGH MICRO AND NANO CAPILLARIES

Ali M. Koupaei
Energy Systems Design Laboratory
Department of Mechanical Engineering
University of Alberta
Edmonton, Alberta, T6G 2G8
CANADA
Email: amkoupaei@ualberta.ca

Sushanta K. Mitra
Micro and Nano Scale Transport Lab.
Department of Mechanical Engineering
University of Alberta
Edmonton, Alberta, T6G 2G8
CANADA
sushanta.mitra@ualberta.ca

Marc Secanell*
Energy Systems Design Laboratory
Department of Mechanical Engineering
University of Alberta
Edmonton, Alberta, T6G 2G8
CANADA
secanell@ualberta.ca

ABSTRACT

Multicomponent mass transport in the micro/nano scale is one of the most important phenomena in many engineering processes such as fuel cells. Therefore, a through understanding of the underlying physics and modeling techniques for mass transport is of crucial importance. According to Kerkhof et al. [1], due to the approximations made in the derivation of the classic transport equations for diffusion-convective dominated problems, the commonly used approach of modeling these problems by the Maxwell-Stefan and Navier-Stokes equations results in trends that are contrary to experiments even for elementary problems like gaseous counter diffusion in capillaries. A new formulation to model molecular fluid transport in multi component systems is then presented. The main aim of this study is to develop a combined experimental-numerical program to study the validity of the classical and the proposed formulations. We discuss the development of an in-house written C/C++ Object Oriented program that solves the classical and recently presented formulation numerically.

1 INTRODUCTION

Numerous authors have developed modeling equations for multicomponent mass transport in porous media and capillaries, the most popular ones being the Dusty Gas Model (DGM) introduced by Evans et. al [2, 3] and Mean Pore Transport Model (MPTM) associated with the works of Rothwell [4], Schneider [5], Arnost and Schneider [6] and others. These two theories are based on different physical fundamentals but, interestingly, they yield similar results in most cases. A comparison between DGM and MPTM is made by Jackson [7]. Kerkhof [8] has recently examined the validity of the DGM model and showed that the DGM formulation leads to contradictions for some basic case studies such as the isobaric counter diffusion phenomenon of two gases through a capillary for which the experimental data is available by Remick and Geankoplis [12].

In a series of articles, Kerkhof proposed a modified version of the MPTM model called Binary Friction Model(BFM) and later on derived another new version of the MPTM called the Velocity Profile Model (VPM) [9]. Finally, in reference [1], he presented a new multicomponent mass transport formulation based on the Boltzman equation. Young and Todd [10] have also suggested a new mass transport model based on the MPTM named the Cylindrical Pore Interpolation Model (CPIM).

Given the multitude of recently proposed mass transport formulations in the literature, a numerical solver capable of implementing these new formulations is necessary. The goal of this research is to develope an object-oriented multicomponent mass transport solver that is capable of solving Fick's mass transport,

*Address all correspondence to this author.

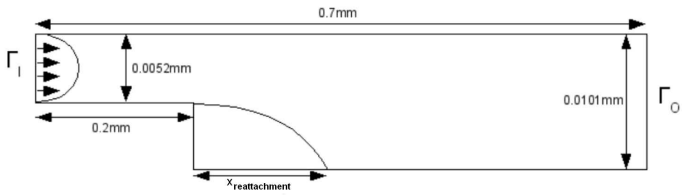

FIGURE 1. SCHEMATICAL CONFIGURATION OF THE CONSIDERED BACKWARD-FACING STEP FLOW PROBLEM

the DGM mass transport, and the Kerkhof mass transport model in order to be able to compare their predictions in a diffusion bridge experiment. These results will also be compared with experiments from Pant et al. [11]. Since implementing Kerkhof's formulation involve solving one Navier-Stokes (N-S) equation per species, first a N-S solver has been implemented and coupled with Fick's law.

In this paper, we discuss the fluid flow solver and a mass tranport solver implementing convection and binary Fickian diffusion as the initial steps towards the development of the aforementioned multi-component mass transport framework. Section 2 presents the results obtained by the fluid flow solver for the backward-facing step problem. These results from the developed code are validated against the experimental data published by Armaly et al. [13]. In section 3, the continuity and momentum equations as well as mass transport governing equations are solved for a diffusion bridge experimental setup. In the final paper, we will discuss the implementation of the recently proposed general model by Kerkhof et al.

2 FLUID FLOW SOLVER

This section presents the development and validation of the fluid flow solver that will be latter coupled with the mass transport equations.

2.1 BACKWARD-FACING STEP FLOW PROBLEM

In order to validate the predictions of the in-house object oriented code, a backward facing step is used as a benchmark test for the incompressible fluid flow solver. This problem is one of the most commonly used benchmark problems in the literature [18]- [21] . Here we will use the code to solve this problem and compare the obtained results with an experimental study conducted elsewhere [13]. Figure 1 depicts the physical domain for this problem as per Armaly et al. experimental setup.

A critical parameter in backward-facing step problems is the reattachment length X (Figure 1). This parameter is the defined as the location at which the velocity axial component changes sign with respect to its initial sign at the step region. This is the region where flow separation takes place.

2.2 GOVERNING EQUATIONS

The fluid inside the domain is considered to be incompressible holding constant physical properties. The flow is assumed laminar and two dimensional. Under the aforementioned conditions one continuity and two momentum balancing equations (in symbolic notation) can be written as,

$$\begin{cases} (\mathbf{v}\cdot\nabla)\mathbf{v} = -\nabla p + \nu\nabla^2\mathbf{v} \\ \nabla\cdot\mathbf{v} = 0 \end{cases} \tag{1}$$

where $\mathbf{v} = (u, v)$ is the velocity, p the pressure and ν stands for kinematic viscosity.

2.3 BOUNDARY CONDITIONS

The boundary conditions for the step flow problem are as follows,

$$\begin{cases} \mathbf{v} = v_{inlet} \times f(x) & on\ \Gamma_I \\ \mathbf{v} = 0 & on\ \Gamma_{Walls} \\ p = \frac{\partial \mathbf{v}i}{\partial \mathbf{x}_j} = 0 & on\ \Gamma_{Outlet} \end{cases} \tag{2}$$

According to the problem domain, sketched in Figure 1, Γ_I, Γ_O and Γ_W are boundary indicators for inlet, outlet and wall regions respectively. As is depicted, a fully developed inlet velocity is introduced into the domain inlet. Hence, $f(x)$ is a polynomial function of order two which ensures the values of zero and one at inlet corners and middle point respectively. This way we would impose a velocity magnitude of v_{inlet} at the middle and zero wall velocity at the channel inlet points.

2.4 OBJECT ORIENTED FINITE ELEMENT SOLVER

The object-oriented code is developed in C++ using the state-of-the-art deal.II finite element library [17]. The PDE system (1) subjected to the boundary condition 2 are discretized using Bubnov-Galerkin finite element scheme [14]. To discretize the solution, second order Lagrange elements are used for the velocity and first order Lagrange elements are used for pressure in order to meet the LBB condition [15]. The convection terms are nonlinear. In this study, Picard method iteration of successive substitution is used to solve the nonlinear equations. According to this scheme, the solution at the n^{th} iteration is determined as,

$$\left[K\left(\{U\}^{(n-1)}\right)\right]\{U\}^{(n)} = \{F\} \tag{3}$$

in which $\{F\}$ is the forcing vector and the coefficient matrix $[K]$ is evaluated by use of the already calculated solution at the

$(n-1)^{th}$ iteration. So the coefficient matrix $[K]$ must be invertible after introducing the boundary conditions. Hence, the initial guess, $\{U\}^{(0)}$ must satisfy the essential (Dirichlet) boundary condition and be such that the coefficient matrix is invertible [16]. The resulting algebraic equations in the matrix form are solved by the freely distributed code, UMFPACK [22] which is an Unsymmetric MultiFrontal method written in ANSI/ISO C.

2.5 INLET/OUTLET LENGTHS EFFECTS

By introducing a fully developed profile at the inlet, it is possible to make the computational domain smaller and make the inlet region effects ignorable. As a consequence, the computational time for the hydrodynamic simulation will decrease dramatically due to smaller number of elements needed to discretize the domain. Several solutions have been obtained with different domains having various enterance lengths and the independent behavior of the solution with respect to various enterance lengths was observed. Since the governing system of equations (1) are hyperbolic, both inlet and outlet regions have definite effects upon the solution. Hence before embarking upon using the solver for analysing the problem an exhaustive procedure for making the solution independent of the inlet/outlet regions is mandatory.

Figures 2 and 3 depict the reattachment length versus various inlet/outlet lengths. As is obvious, the target solution parameter, the reattachment length versus step length $\frac{X}{S}$, becomes independent of the enterance lenght and the outlet of the channel. Any domain having enterance lengths not less than 15 *mm* and outlet length not less than 150 *mm* can be employed and discretized with much lower number of elements to study this problem taking lesser computational time as well.

2.6 MESH SENSITIVITY STUDY

In order to obtain results which are independent of the grid total number of cells, a grid sensitivity study was performed. The grid is chosen to be uniform throughout the domain.

According to the finite difference scheme employed by Armaly et al. [13], the required number of grid points for a solution to be grid-independent increases with the Reynolds number. Since this study is concern with flows with Reynolds numbers up to 400, a grid that can provide a grid-independent solution for a Reynolds number of 400 is used in all the studies presented. The nondimensional reattachment length for various grids at a Reynolds number of 400 is obtained starting from a coarse grid and continuing up until the obtained length becomes constant with respect to the grid total cell number. The results are plotted against the total number of cells in Figure 4. According to the obtained results a grid with 59,136 quadrilateral elements is chosen for the rest of the calculations.

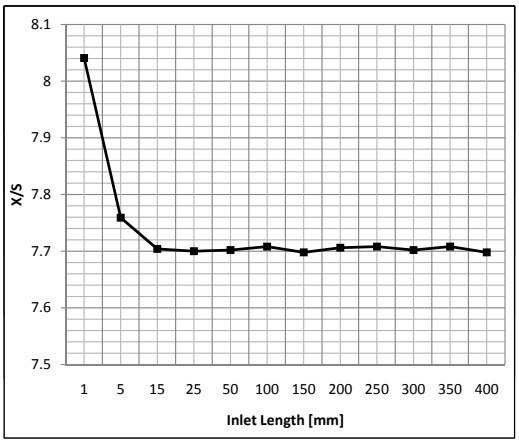

FIGURE 2. EFFECT OF INLET LENGTH ON THE SOLUTION FOR BACKWARD-FACING STEP PROBLEM.

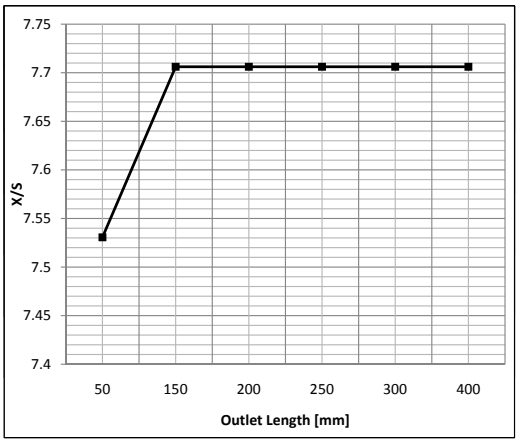

FIGURE 3. EFFECT OF OUTLET LENGTH ON THE SOLUTION FOR BACKWARD-FACING STEP PROBLEM.

2.7 BACKWARD-FACING STEP PROBLEM RESULTS AND VALIDATION

In order to estimate the validity of the code, the reattachement lenght at various Reynolds numbers is predicted using the developed numerical code. The length at which this separation occurs, i.e. the reattachment lenght, can be measured via a plot of the axial velocity component versus the length after the step region. Kitware Paraview 3.6.2 [23] is used for post processing. A plot of the pathlines for the step problem at the step region is

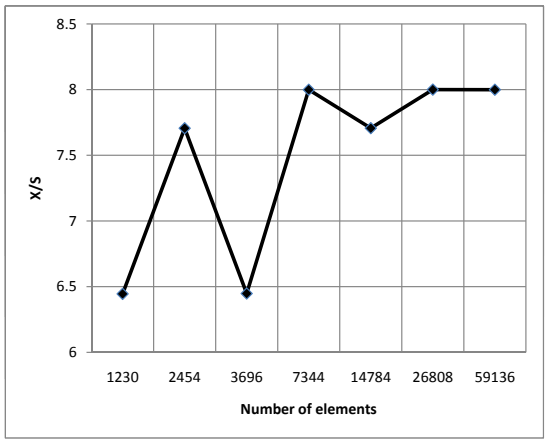

FIGURE 4. EFFECT OF GRID ON THE SOLUTION FOR BACKWARD-FACING STEP PROBLEM (RE=400).

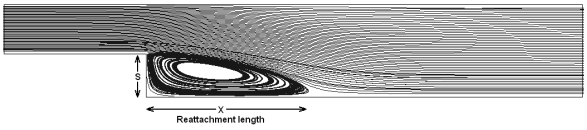

FIGURE 5. PATH LINES FOR BACKWARD-FACING STEP PROBLEM AT RE=125.

in Figure 5. The Reynolds number is calculated via the following formulation,

$$Re = \frac{\mathbf{v}D}{\nu} \tag{4}$$

in which,

$$\nu = \frac{\mu}{\rho} = \frac{18.20755 \times 10^{-6}}{1.205} = 15.11 \times 10^{-6} \left[\frac{m^2}{sec}\right] \tag{5}$$

is the kinematic viscosity defined by dynamic viscosity, μ and density, ρ. Physical properties has been chosen for air at 20^oC. The calculation of Re is based on the $\frac{2}{3}$ of the measured maximum inlet velocity and D is the hydraulic diameter of the channel inlet; namely twice inlet height. So accounting for $Re = 50$ reads,

$$Re = 50 = \frac{\frac{2}{3}u_{inlet}}{15.11 \times 10^{-6}} \times 2 \times 5.2 \times 10^{-3} \tag{6}$$

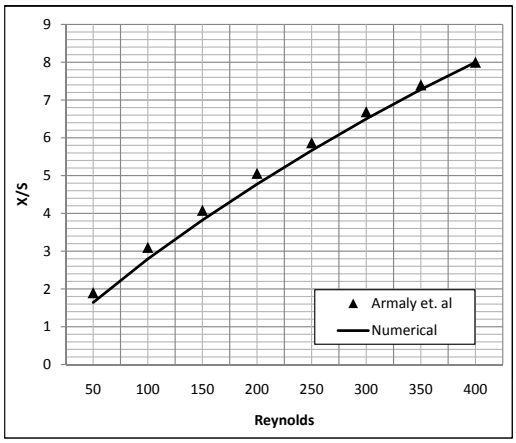

FIGURE 6. REATTACHMENT LENGTH FOR VARIOUS REYNOLDS NUMBER.

Then, we can calculate u_{inlet} which afterwards can be prescribed as inlet velocity to the channel. In this study, numerical runs are performed for flows of Reynolds number up to 400. Furthermore, after this Reynolds number the experimental and numerical results start deviating which are due to the three dimensionality trait of the flow after this Reynolds values [13].

According to Armaly et al.'s numerical and laboratory experiments [13], the reattachment length increases as Reynolds number increases. The reattachment length predicted by Armaly et al. and by the developed fluid flow solver at various Reynolds numbers are plotted in Figure 6. Figure 6 shows that the results obtained from the code are in very good agreement with the experimental results obtained by Armaly et al. [13]. Hence, the implemented fluid flow solver code has reproduced the experimental data for the case of two dimensional laminar and incompressible flow of air over the backward-facing step.

3 MASS TRANSPORT SOLVER

This section presents the results of a convetion-diffusion in-house solver. This solver will be used to study the effect of convection in a capillary diffusion bridge. In the future, this solver will be used to compare the predictions of the classical mass transport formulations to the newly proposed formulation by Kerkhof et al. [1].

3.1 GOVERNING EQUATION

In this section, the Fick's law of diffusion is introduced to account for the mass transfer flux of the species in a binary ideal gaseous solution of Nitrogen and Oxygen. For simplicity, con-

stant physical properties including total viscosity and density are considered for the binary mixture throughout the domain. The governing equation of the convection-diffusion problem are,

$$\begin{cases} (\mathbf{v}\cdot\nabla)\mathbf{v} = -\nabla p + \nu\nabla^2\mathbf{v} \\ \nabla\cdot\mathbf{v} = 0 \\ \nabla\cdot N_1 = 0 \qquad\qquad in\ \Omega \end{cases} \tag{7}$$

where N_1 is the mass transfer flux for the first component and is defined as,

$$\nabla\cdot N_1 = \mathbf{v}\cdot\nabla C_1 - D\nabla^2 C_1 \quad in\ \Omega \tag{8}$$

where C_1 is the molar concentration of the first component. Assuming that the gas behavies as an ideal gas,

$$C = \frac{P}{RT} \tag{9}$$

and after arrangement and simplification for the concentration of the species, the last equation of the system of PDEs (7) reads,

$$\begin{cases} \mathbf{v}\cdot\nabla p_1 = D\nabla^2 p_1 \ in\ \ \Omega \\ p_1 = 101.3kPa \quad on\ \Gamma_{Inlet} \\ \nabla p_1 = 0 \qquad on\ \Gamma_{Outlet} \end{cases} \tag{10}$$

in which p_1 is the pressure of the species number one. According to this terminology, the mole fraction can be obtained as $\frac{p_1}{p^t}$.

3.2 PHYSICAL DOMAIN AND BOUNDARY CONDITIONS

The physical domain and sizes for the channel under consideration is depicted in the Figure 7. The domain is composed of two main channels which have been connected to each other via a micro capillary of 0.5mm height and 50 micron width.

A fully developed velocity profile is imposed for the inlets to the main channels. Total pressure at both the outlets is imposed to be zero. For the lower channel, a pressure of 101.3kPa is imposed for Oxygen and on the upper channel the pressure for Nitrogen is set to 101.3kPa. This will render the partial pressures for Oxygen and Nitrogen on the lower channel inlet to zero.

Taking into account the micro capillary diameter, the assumption of Knudsen flow does not hold $(K_n < 1)$. Therefore, the velocity and diffusion slip phenomena [24] are ignored and a no-slip boundary condition is used to describe the flow at the walls for both species.

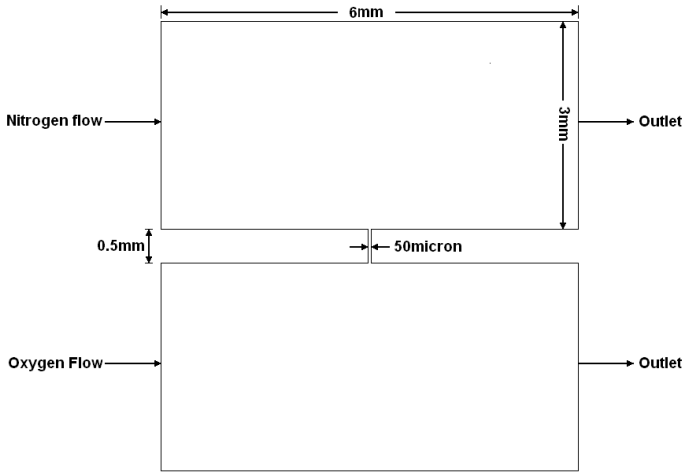

FIGURE 7. THE PHYSICAL DOMAIN AND CHANNEL SIZES FOR THE MICRO CHANNEL PROBLEM.

3.3 COMPUTATIONAL MESH

According to the problem domain size in Figure 7 a more refined mesh is necessary in the capillary due to higher field variable gradient in this region. Therefore, an adaptive mesh refinement strategy is considered to: a) enhance the solution convergence, and b) accelerate the solution process. Starting from a very coarse mesh over the domain, adaptive mesh refinement is used. The mesh used in this study is shown in Figure 8. An expanded view of the micro capillary mesh is also provided. As is well depicted, near capillary wall, inlet-to and outlet-from regions are refined. By using hanging nodes, a mesh with high levels of refinement in the capillary and large elements in the channels can be obtained.

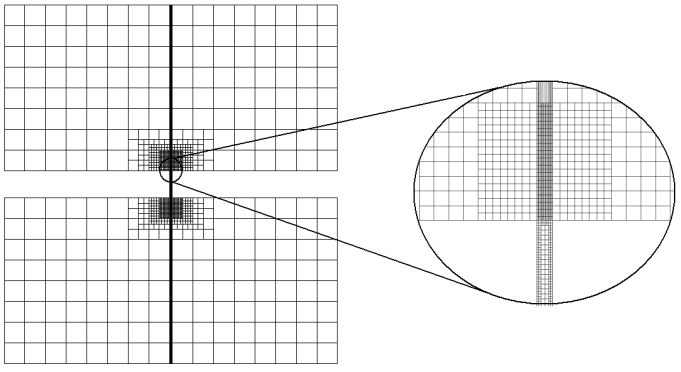

FIGURE 8. THE ADAPTIVE GRID REFINEMENT FOR THE CHANNEL PROBLEM.

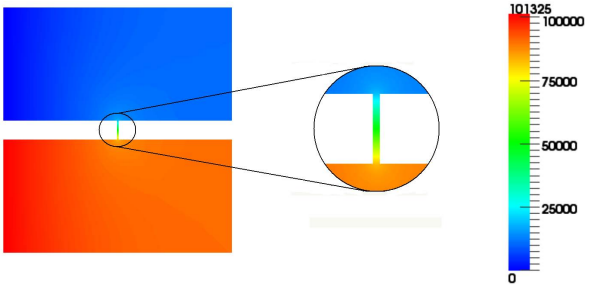

FIGURE 9. OXYGEN PRESSURE PROFILE ALONG A 50 MICRON CAPILLARY AT RE=1.

3.4 NUMERICAL SOLUTION

To solve the equation for the balance of the species, equation (10) is discretized using weighted residual method [14] and first order Lagrange elements for p_1. Because of convective terms in the equation, we need to have the velocity vectors everywhere in the domain to solve for the species mass transport. Hence the velocity terms in the above equation are treated as known parameters from the fluid flow solver. Accordingly, the program solves for the N-S equation and then the results will be used to solve for the species mass balance throughout the domain in a coupled manner. Namely, from the implementational point of view, the code solves both N-S and species mass tranport equations simultaneously within a unified system of equations but from the computational point of view these equations are decoupled because the velocity terms in the species mass transpport equation are treated as known parameters. Hence as mentioned before, for solving the species transport equation, velocity components are necessary to be known.

3.5 CHANNEL AND MICROCHANNEL RESULTS

Employing the already implemented and validated fluid flow solver, the mass transport equation 10 together with the system of continuity and momentum balancing PDEs (1) subjected to the introduced boundary conditions can be numerically solved. The pressure profile for Oxygen is plotted in Figure 9. The Oxygen flow at the lower channel and Nitrogen at the upper channel poses a counter diffusion process to occur through the connection by the micro capillary. Hence, the decreasing trend in the Oxygen pressure from the lower channel towards the upper one is apparent and is evident in the Figure 9.

Propagation of Oxygen through micro capillary into the other big channels is apparent from the Figure 9. As a result of Oxygen diffusion through the micro capillary, the Oxygen pressure decreases along the capillary all the way to the upper channel where gaseous pure Nitrogen flows from left to right. In addition, because of Nitrogen zero pressure at the lower channel where pure Oxygen flows, there is another diffusion phenomenon

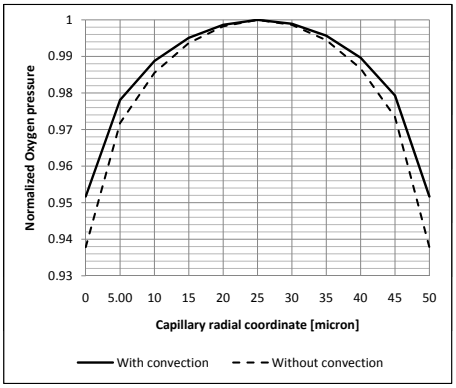

FIGURE 10. NORMALIZED RADIAL OXYGEN PRESSURE PROFILE AT THE CAPILLARY OUTLET TO THE UPPER CHANNEL (RE=1).

in the opposite direction from the upper channel towards the lower one through the capillary connection. So therefore, there a counterdiffusion process exists until the species partial pressures at both channels become the same.

Nitrogen pressure can be calculated via,

$$p_{total} = p_{O_2} + p_{N_2} \tag{11}$$

where the first two pressures, p_{total} and p_{O_2}, are calculated by the solver.

Figure 10 shows the effect of convection upon the Oxygen concentration at the capillary outlet to the upper main channel. As can be seen in the plot, the Oxygen concentration at the capillary outlet is considerably higher when convection is taken into account in the convection-diffusion equation in comparison to when covection is ignored. As a result, the average amount of Oxygen transported through the micro capillary towards the upper channel where pure Nitrogen is flowing is more.

Viscosity of gases and mixtures change with concentration and various models have been proposed to calculate viscosities [25]. Since the viscosity of Oxygen ($23.7 \times 10^{-6} pa.sec$) and Nitrogen ($20.7 \times 10^{-6} pa.sec$) are not considerably different from each other, using Wilke's method, to calculate the viscosity of a mixture composed of 50% (by mole Oxygen) and 50% Nitrogen, reveals that the mixture viscosity ($22.2 \times 10^{-6} pa.sec$) is close to the individual components' viscosities. This is while, numerical results show less than 5% difference when using pure Oxygen, pure Nitrogen or mixture viscosity values.

4 CONCLUSIONS AND FUTURE WORK

The incompressible isothermal and laminar flow of gas through two dimensional domain is implemented and described. The Navier-Stokes solver is validated against experimental data for the case of backward-facing step problem. Very good agreement with the experimental results of Armaly et. al was achieved. Also the Fick's law of diffusion to account for the species mass transport through the microchannel was implemented and the results obtained for the Oxygen pressure profile through the micro capillary. Furthermore, an optimized adaptive grid was introduced for the channel problem. Future work will include the proposed Kerkhof model for describing the species transport through micro and nano capillaries.

Because density changes with concentration, we would need to solve the compressible version of the Navier-Stokes equations to account for the density changes due to concentration. The goal of the project is to develop a fluid flow solver that is open source and allows others to easily implement mass transport formulations. As a first step, authors have decided to start from the simplest form and that is why constant properties are assumed for now. Solution of the compressible version of the N-S equations is planed for the future work. Besides, although density of Oxygen ($1.30\frac{kg}{m^3}$), Nitrogen ($1.13\frac{kg}{m^3}$) and a binary mixture of them ($1.21\frac{kg}{m^3}$) are close to each other, again numerical runs show very small difference between the results obtained by using pure Oxygen density or pure Nitrogen density or mixture density.

In order to validate the numerical framework with respect to experimental data, a diffusion bridge experimental setup is being developed in parallel [11]. Future work will focus on modeling the exact geometry of the experimental setup and comparing numerical and experimental results. This comparison will provide insight on the validity of various mass transport formulations.

REFERENCES

[1] Kerkhof, P., and Geboers, M., 2005. "Toward a unified theory of isotropic molecular transport phenomena". *AIChE Journal,* ***51***(1), pp. 79–121.

[2] Evans , R.B., Watson, G.M., Mason, E.A., 1961. "Gaseous diffusion in porous media at uniform pressure". *The Journal of Chemical Physics,* ***35***(6), pp. 2076–2083.

[3] Evans , R.B., Watson, G.M., Mason, E.A., 1962. "Gaseous diffusion in porous media. II. Effect of pressure gradients". *The Journal of Chemical Physics,* ***36***(7), pp. 1894–1902.

[4] Rothwell, L. B., 1963. "Gaseous counterdiffusion in catalytic pellets". *American Institute of Chemical Engineering Journal,* ***9***, pp. 19–24.

[5] Schneider, P., 1978. "Multicomponent isothermal diffusion and forced flow of gases in capillaries". *Chemical Engineering Science.,* ***33***(10), pp. 1311–1319.

[6] Arnost, D., Schneider, P., 1995. "Dynamic transport of multicomponent mixtures of gases in porous solids". *The Chemical Engineering Journal and The Biochemical Engineering Journal.,* ***57***(2), pp. 1311–1319.

[7] Jackson, R., 1977. "Transport in Porous Catalyst". *Chemical Engineering Monographs.,* ***4***, pp. 1311–1319.

[8] Kerkhof, P.J.A.M., 1996. "A modified Maxwell-Stefan model for transport through inert membranes: The binary friction model". *Chemical Engineering Journal and the Biochemical Engineering Journal.,* ***64***(3), pp. 319–343.

[9] Kerkhof, P.J.A.M., Geboers, M.A.M., Ptasinski, K.J., 2001. "On the isothermal binary mass transport in a single pore". *Chemical Engineering Journal.,* ***83***(2), pp. 107–121.

[10] Young, J.B., Todd, B., 2005. "Modeling of multicomponent gas flows in capillaries and porous solids". *International Journal of Heat and Mass Transfer.,* ***48***, pp. 25–26.

[11] Pant, L., Secanell, M., Mitra, S., 2010. "Design of an Experimental Setup To Study Mass Transport In Micro-Nano Capillaries And Porous Media". *Submitted* in International Conference on Nanochannels, Microchannels, and Minichannels, Montreal, Canada, no. FEDSM-ICNMM2010-30305, ASME.

[12] Remick, R.R., Geankoplis, C.J., 1973. "Binary diffusion of gases in capillaries in the transition region between Knudsen and molecular diffusion". *Industrial and Engineering Chemistry,* ***12***(2), pp. 214–220.

[13] Armaly, B.F., Durst, F., Pereira, J.C.F., Schoenung, B., 1983. "Experimental and Theoretical Investigation of Backward-Facing Step Flow". *Journal of Fluid Mechanics,* ***127***, pp. 473–496.

[14] Reddy, J. N. , 1993. "An Introduction to the Finite Element Method". *McGraw-Hill, Inc.*

[15] Donea, J., Huerta, A., 2003. "Finite Element Method for Flow Problems". *John Wiley and Sons, Ltd.*

[16] Reddy, J. N. , 2004. "An Introduction to Nonlinear Finite Element Analysis". *Oxford University Press.*

[17] Website : http://www.dealii.org

[18] Prabhakar, V., Pontaza, J.P., Reddy, J.N., 2008. "A collocation penalty least-squares finite element formulation for incompressible flows". *Comput. Methods Appl. Mech. Engrg.,* ***197***, pp. 449–463.

[19] Hughes, T. J. R. , Liu, W. K. , Brooks, A., 1979. "Finite Element Analysis of Incompressible Viscous Flows by the Penalty Function Formulation". *Journal of Computational Physics.,* ***30***, pp. 1–60.

[20] Gresho, Philip M. , Gartling, D. K. , Torczynski, J. R., Cliffe, K. A., Winters, K. H., Garratt, T. J., Spence, A. , Goodrich, J. W., 1993. "Is The Steady Viscous Incompressible TwoDimensional Flow Over A Backward0Facing Step At Re = 800 Stable?". *International Journal For Numerical Methods In Fluids.,* ***17***, pp. 501–541.

[21] Pereira, V. D. , Campos Silva, J. B. , 2005. "Simulations

of Incompressible Fluid Flows by a Least Squares Finite Element Method". *J. of the Braz. Soc. of Mech. Sci. and Eng.,* ***27***(3), pp. 274–282.
[22] Website : http://www.cise.ufl.edu/research/sparse/umfpack
[23] Website : http://www.paraview.org
[24] Kramers, H.A., Kistemaker, J., 1943. "On the slip of a diffusing gas mixture along a wall". *Physica.,* ***10***(8), pp. 214–220.
[25] Poling, B. E., Prausnitz, J. M., O'Connell, J. P., 2001. "The Properties of Gases and Liquids". *McGraw-Hill, Inc.*